buildings

MDPI

Article

Study on Dynamic Response of Inclined Pile Group Foundation under Earthquake Action

Weihong Huang [1], Jiankun Liu [1], Heng Wang [2,*], Mo'men Ayasrah [3,*], Hongsheng Qiu [2] and Zhuofan Wang [2]

[1] School of Civil Engineering, Sun Yat-Sen University, Guangzhou 510275, China; huangwh76@mail2.sysu.edu.cn (W.H.); liujiank@mail.sysu.edu.cn (J.L.)
[2] School of Transportation and Logistics Engineering, Wuhan University of Technology, Wuhan 430063, China; 2755@whut.edu.cn (H.Q.); 333133@whut.edu.cn (Z.W.)
[3] Department of Civil Engineering, Faculty of Engineering, Al al-Bayt University, Mafraq 25113, Jordan
* Correspondence: 305467@whut.edu.cn (H.W.); ayasrahmomen@aabu.edu.jo (M.A.)

Abstract: With the development of all types of new special-shaped arch bridges, the deformation of the pile foundation of special-shaped steel arch bridges has a great influence on the superstructure, and the requirements for it are strict. In addition, the force of the inclined pile group under an earthquake is complicated. In this paper, based on the Zhuhai Jindao Bridge project, the finite element numerical model is established in order to study the dynamic response and parameter influence law of an inclined straight pile group foundation under earthquake action. After a thorough analysis of the results of the simulation, it was found that under the action of an earthquake, the inclination angle of inclined piles has a significant influence on the seismic ability of pile group foundations. When the inclination angle of an inclined pile is 5°, the ability of the inclined pile group foundation to resist deformation can be effectively improved, and the load distribution of the pile top is more reasonable.

Keywords: inclined pile; finite element analysis; dynamic characteristics; seismic response

check for updates

Citation: Huang, W.; Liu, J.; Wang, H.; Ayasrah, M.; Qiu, H.; Wang, Z. Study on Dynamic Response of Inclined Pile Group Foundation under Earthquake Action. *Buildings* **2023**, *13*, 2416. https://doi.org/10.3390/buildings13102416

Academic Editor: Bartolomeo Pantò

Received: 28 July 2023
Revised: 6 September 2023
Accepted: 19 September 2023
Published: 22 September 2023

Copyright: © 2023 by the authors. Licensee MDPI, Basel, Switzerland. This article is an open access article distributed under the terms and conditions of the Creative Commons Attribution (CC BY) license (https://creativecommons.org/licenses/by/4.0/).

1. Introduction

With the continuous updating of urban infrastructure, special-shaped steel arch bridges with unique shapes have gradually become an important choice for urban architecture. Complex structures put forward new requirements regarding the force of pile foundations. An inclined straight pile group foundation consists of inclined and straight piles, and its working mechanism is different from that of conventional pile foundations. When inclined piles participate in bearing lateral loads in the pile group, the displacement of the pile top and the internal force of the pile body are reduced by varying degrees, making inclined straight piles more suitable for arch bridge foundations [1,2]. The dynamic response law of inclined straight pile groups under earthquake action is complex [3]. Currently, there is a lack of seismic design provisions for inclined straight pile groups in seismic design specifications. Therefore, it is necessary to conduct research on the dynamic response of inclined straight pile groups.

The bearing capacity and seismic performance of inclined pile groups have been paid attention to by geotechnical engineering researchers. The research methods of inclined piles mainly include laboratory tests [4–8] and numerical calculations [9–15]. Some scholars also analyzed inclined piles using the p–y curve method. Zhou Dequan et al. [16] set an inclined pile at different angles in the model sand and applied a horizontal load to the top of the pile, so as to obtain the change law of p–y curve characteristics with the inclination angle and pile bottom constraint conditions. Chen Wenlong et al. [17] carried out a vibration table comparison test of inclined and straight piles in saturated sand and discussed the seismic performance of inclined pile foundations from three aspects: superstructure acceleration, pile top shear force and the pile body bending moment. In recent years, many scholars have carried out studies on the seismic performance of inclined pile foundations through

numerical simulation [17–22]. Ref. [23] obtained peak cap acceleration and displacement based on a shaking table test and compared them with FLAC-3D numerical simulation. The results show that FLAC-3D software is able to better simulate the dynamic response of inclined piles. In this paper, focusing on the stress characteristics of the inclined pile group and relying on a real-life engineering scenario, the finite element software MIDAS Civil was used to establish a three-dimensional model, and the time-history analysis method was used to analyze the seismic response of inclined pile group foundations.

The special-shaped arch bridge studied in this paper is a separate arch rib structure, and the stress and parameter influence rules during earthquakes are different from those of conventional arch bridges, resulting in a complicated load transfer to the pile foundation. Therefore, based on the stress characteristics of the special-shaped arch bridge studied in this paper, the stress conditions and deformation rules of the inclined straight pile group structure of an arch bridge were analyzed. Relying on a real-life engineering scenario, the finite element software MIDAS Civil was used to establish a three-dimensional model and verify the rationality of the model. On this basis, the seismic response analysis of the inclined straight pile group foundation was carried out using the time–history analysis method. This provides a reference for the design of inclined pile groups for this type of special-shaped arch bridge in practice.

The remainder of this paper is organized as follows. Section 2 presents the details of the engineering scenario. In Section 3, the establishment of the finite element model is explained. The analysis of natural vibration characteristics is shown in Section 4. The computational results are presented and analyzed in Sections 5 and 6, respectively. Finally, Section 7 presents the conclusions.

2. Engineering Scenario

2.1. Project Profile

The Jindao Bridge is located in Jinwan District, Zhuhai. The arch rib is a separate structure. After the completion of the bridge, it will become a beautiful part of the scenery in Zhuhai with its beautiful and unique shape. The bridge spans the main flood drainage channel. The starting point of the bridge is KC0 + 132.00, and the endpoint of the bridge is pile number KC0 + 232.00. An asymmetrically shaped arch bridge structure was adopted. A 3D render of the Golden Island Bridge is shown in Figure 1.



Figure 1. A 3D render of the Golden Island Bridge.

2.2. Superstructure Profile

The total width of the bridge is 46.25 m, and the main beam is a steel–concrete composite beam structure. Three box longitudinal beams are set on the main beam. The top and bottom of the side longitudinal beams are the same as the bridge floor, and the

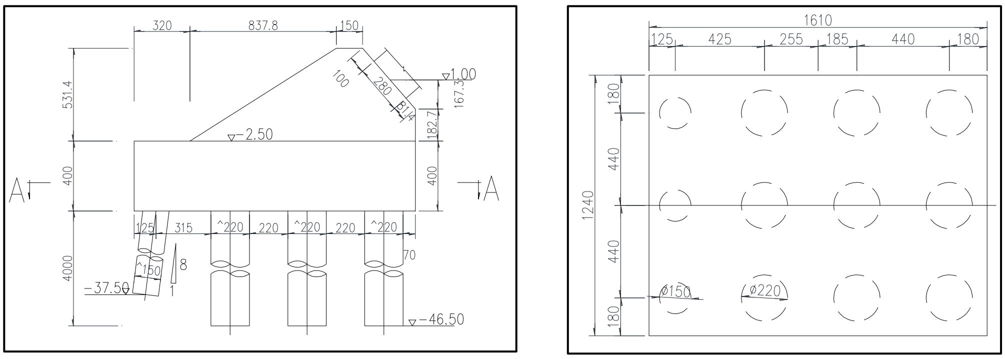
transverse slope is 1.5% inward. The width of the side longitudinal beams is 2.0 m, and the height is 1.5 m. The longitudinal beam is provided with a transverse partition every 4 m, and a steel beam is located between the longitudinal beam of the side box and the longitudinal beam of the middle box. The beam spacing is 4.0 m, and the beam is part of a "working" section. The thickness of the upper and lower flanges is 24 mm, the thickness of the web is 12 mm, the height of the end beam is 1.5 m, the thickness of the upper and lower flanges is 30 mm, and the thickness of the web is 20 mm. A small longitudinal beam is arranged in the middle of the span between the beams. The small longitudinal beam consists of an I-section, the beam height is 0.7 m, the thickness of the upper and lower flanges is 16 mm, and the thickness of the web is 12 mm.

In addition, the arch rib is connected with the main beam via a derrick. The derrick comprises 19 × Φs15.24; 27 × Φs15.24; and 37 × Φs15.24 types, whose tensile strength is no less than 1860 MPa. The distance between the derrick and the bridge is 4.0 m. The wind support utilizes a Φ630 × 16 mm seamless steel pipe.

The theoretical span of the No.1 to No.3 arch ribs is 128.125 m, 110.0 m, and 128.125 m; the vector height is 44 m, 40 m, and 44 m; and the vector span ratio is 1/2.91, 1/2.75, and 1/2.91, respectively. The section outline dimensions of arch ribs are 2.8 m × 2.8 m, and the longitudinal section is equal to this section. The main bridge is a steel arch bridge with a span arrangement of 1 × 100 m.

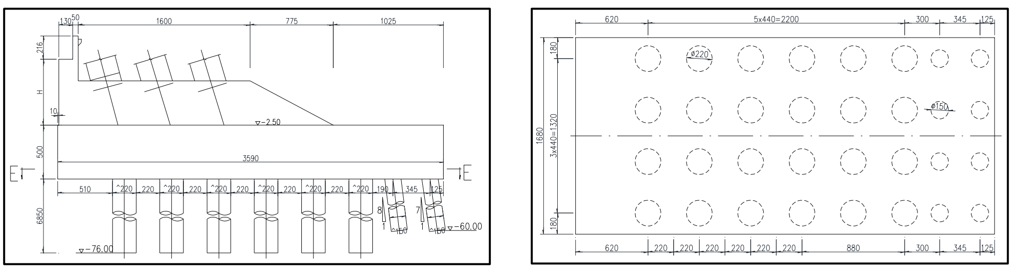
2.3. Pile Foundation Layout Scheme

The arch seat and cap are made of C40 concrete, the cap is rectangular, the size of the #1–3 arch seat cap is 12.4 × 16.1 m, and the thickness is 4.0 m. Nine boreholes and cast-in piles with diameters of 2.2 m and 3 inclined steel pipe piles with diameters of 1.5 m are used. The size of the #4 arch seat cap is 16.8 × 35.9 m, and the thickness is 5.0 m. Twenty-four drilled cast-in piles with a 2.2 m diameter, and fourteen inclined steel pipe piles with a 1.5 m diameter are used. The #4 arch seat cap is close to the abutment, part of the platform is directly set on the #4 arch seat cap, and a 2 cm fault joint is set between the #4 arch seat and the abutment. The structure diagrams of #1~#4 arch are shown in Figures 2 and 3.



(**a**) (**b**)

Figure 2. The #1~3 arch structure layout: (**a**) elevation of #1~3 arches; (**b**) plan of #1~3 arches.



(**a**) (**b**)

Figure 3. The #4 arch structure drawing: (**a**) elevation of the #4 arches; (**b**) plan of the #4 arches.

3. Establishment of a Finite Element Model

In bridge engineering, when the span of the structure is much larger than the other two dimensions (width and height of the section), it can be approximately simplified to the bar structure in model analysis. A large number of experiments and calculations show that this simplification meets the accuracy requirements of bridge structural analysis [24,25]. In this paper, in order to meet the requirements and accuracy of model analysis and to avoid the memory and time required for calculation, the model is properly simplified, which not only reduces the corresponding calculation amount but also speeds up the research progress.

In the modeling of the whole bridge structure, X and Y were defined as the transverse and longitudinal bridge directions, respectively, and Z is defined as the gravity direction. The structure was transformed into a space rod model, which divided the bare arch state and the bridge stage. The suspender was simulated using a tensile element only. The arch rib, wind support, main beam, arch seat, and pile foundation were simulated using beam element, and the bridge panel was simulated using the plate element. The whole bridge was divided into 2250 nodes and 2830 elements. The numerical model of the bridge is shown in Figure 4. In addition, the relevant material properties used in this model are shown in Table 1.

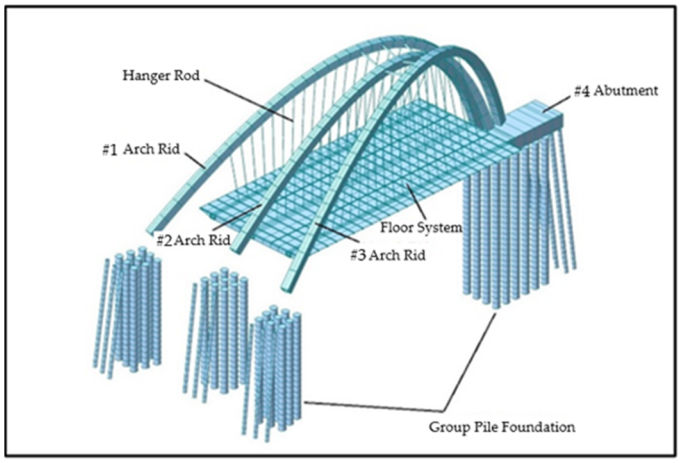


Figure 4. Full bridge model of special-shaped steel arch bridge.

Table 1. Material properties used in the numerical analysis.

Material Name	Type	Elastic Modulus (MPa)	Poisson's Ratio	Unit Weight (KN/m^3)	Linear Expansion Coefficient (1/[C])
Q345	Steel	2.06×10^5	0.3	76.98	1.2×10^{-5}
Strand1860	Steel strand	1.95×10^5	0.3	78.5	1.2×10^{-5}
C40	Concrete	3.25×10^4	0.2	25	1.0×10^{-5}
C30	Concrete	3.0×10^4	0.2	25	1.0×10^{-5}

3.1. Main Beam Simulation

The whole main beam is composed of three main longitudinal beams, spacer beams, and small and medium-sized longitudinal beams across the beam, all of which are simulated via beam elements. Considering the 1.5% transverse slope of the longitudinal beam, the virtual beam is set on both sides, a rigid connection is adopted between the longitudinal beam and the main beam, and a total of six supports are set at both ends of the middle longitudinal beam and the main longitudinal beam. The constraints of the supports are presented in Table 2. All sections were drawn using CAD and imported into Midas/Civil SPC to calculate the section characteristics, to generate the section of each beam body, and then to assign the section and material to the element. The main beam model is shown in Figure 5.

Table 2. Boundary conditions of the supports.

Support Number	X	Y	Z	Rx	Ry	Rz
Support 1	1	1	0	1	1	1
Support 2	0	0	0	1	1	1
Support 3	1	1	0	1	1	1
Support 4	1	1	0	0	0	0
Support 5	1	0	0	1	1	1
Support 6	1	1	0	1	1	1

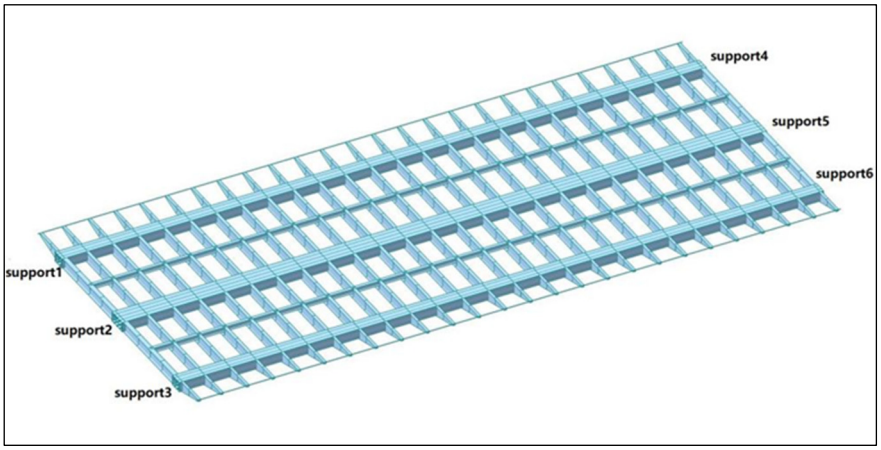


Figure 5. Full bridge model of special-shaped steel arch bridge.

Here, X is the transverse bridge direction, Y is the longitudinal bridge direction, and Z is the vertical bridge direction. In addition, 1 means that the degree of freedom is relaxed, and 0 means that the degree of freedom is constrained.

3.2. Arch Rib and Foundation Simulation

The cross-sections of three types of arch rib segments were drawn in CAD, imported to calculate the section characteristics, and assigned to the section of arch rib. After that, the plane coordinates of the three arch ribs with the steel–concrete junction as the origin were calculated according to the quadratic oblique parabola formula in the design drawing. Since curves cannot be recognized in Midas Civil, multiple distributed arch rib nodes were connected insofar as possible through multiple line segments in CAD to ensure a better arch rib alignment in the modeling. In addition, corresponding nodes were set at the connection between the boom and the main arch. The arch rib and wind-bracing models are shown in Figure 6.

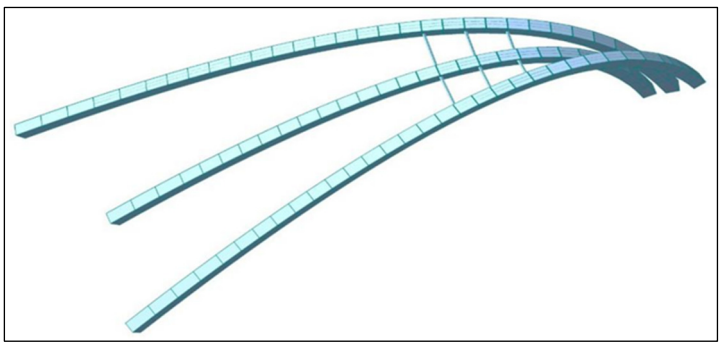


Figure 6. Main arch and wind support model.

Arch #4 is located at the intersection of the three arch ribs, and the force is complicated. In order to make the load distribution of pile foundation more reasonable, a bearing cap is

set at the large arch seat of the model as a transmission medium, and a bearing cap is set at the arch seat #4. The bearing cap is simulated using the beam element, so that the load of the superstructure can be reasonably distributed to pile foundation. A rigid connection is set at the intersection of the three arch feet projected in the Z direction and the simulated cap of the beam unit. The cap and each single row of piles are rigidly connected with the cap as the main node and the top of the pile as the secondary node, so that the load transmitted by the cap is relatively evenly distributed to the pile foundation. For the end of the small arch seat, only the single arch transmits the load. Therefore, the pile top displacement can be reasonably distributed through the direct use of the primary–secondary node connection. The arch foot and pile group at the #1–#3 arch seat are rigid and connected through the "arch main pile slave". In addition, in order to consider the influence of the interaction between piles and soil, the soil spring method is used to simulate the effect of soil on the pile, and the stiffness of the equivalent soil spring is calculated through the "m" method. The pile foundation nodes are simulated using the linear node elastic support. The boundary constraints are shown in Table 3.

Table 3. Arch rib-dependent boundary conditions.

Structure Combination Type	Constraint Condition
Arch rib and wind support	Rigid connection
Arch foot and pile foundation (#1~3 arch seat)	Rigid connection (#1–3 arch seat)
Arch foot and cap (#4 arch seat)	Rigid connection (Z direction)
Cap and pile foundation	Rigid connection (Z direction)
Pile foundation	Linear joint elastic support

Note: The Z direction indicates that the nodes are in the same vertical plane.

3.3. Load Condition

The special-shaped arch bridge is located in Zhuhai City. Besides the general design load, load considerations should be combined with reality. The reasonable consideration of the load condition is more conducive to the fitting of the finite element model to reality. The load types include structural dead weight, secondary dead load, crowd load, automobile load, temperature load, the initial tension of the boom, and wind load. In the finite element model, the self-weight of the structure will be automatically calculated. The load grade of vehicles is decided at city level. According to the General Code for the Design of Highway Bridges and Culverts (JTG D60-2004) [26], the crowd load q = 2.5 kN/m^2, the overall temperature of the whole bridge is calculated according to a temperature rise of 21° and a temperature drop of 29°, and the wind load is considered according to the 100-year-old wind standard of the service stage. The initial tension of the boom is shown in Table 4.

Table 4. Initial pull of the boom.

Modal Order	Boom Tension			Modal Order	Boom Tension		
	#1Arch Rib	#2Arch Rib	#3Arch Rib		#1Arch Rib	#2Arch Rib	#1Arch Rib
1	30	30	30	11	120	140	120
2	30	50	30	12	120	140	120
3	100	100	135	13	120	160	120
4	135	160	135	14	120	160	120
5	135	160	135	15	120	180	120
6	135	140	135	16	150	200	120
7	135	140	135	17	180	200	180
8	135	140	120	18	150	200	150
9	135	140	120	19	150	100	150
10	120	140	120	20	150	30	120

4. Analysis of Natural Vibration Characteristics

The premise of the study of dynamic problems is the calculation of the dynamic characteristics of the structure, including the natural vibration frequency and vibration type of the structure and so on. Each natural vibration mode has a fixed frequency, damping ratio, and shape, and its calculation results are the foundation of seismic analysis. The purpose of modal analysis is to avoid certain external excitations (such as earthquakes, crowds, and wind vibrations) approaching the natural frequency of the structure during structural design, thereby preventing resonance and vibration phenomena in the structure. This allows for a more comprehensive analysis of how the structure responds to different types of dynamic loads, which is beneficial for solving and calculating control parameters in other dynamic analysis.

The principle of modal analysis is based on the undamped free vibration equation. The structure is discretized into a calculation model of finite degrees of freedom, ignoring the influence of structural damping [27]. In this case, the damping matrix and the node load matrix are equal to 0, and the undamped free vibration equation of the structure is as follows:

$$[M]\left\{\ddot{X}\right\} + [K]\{X\} \tag{1}$$

where $[M]$ is the structure mass matrix, $[K]$ is the structural stiffness matrix, $\left\{\ddot{X}\right\}$ is the structural acceleration vector, and $\{X\}$ is the structural displacement vector.

Hypothetical order:

$$\{X\} = \{Ø\}sin(\omega t + \varphi) \tag{2}$$

Then, there is:

$$\left\{\ddot{X}\right\} = -\omega^2\{Ø\}sin(\omega t + \varphi) \tag{3}$$

where ω is the vibration frequency, t is the time, φ is the phase angle, and Ø is the displacement amplitude vector that does not change with time.

Hypothetical order:

$$\mu = \omega^2 \tag{4}$$

The Formulas (2)–(4) can be substituted into Formula (1), so that the final arrangement can be obtained:

$$([K] - \mu[M])\{\varphi\} = \{0\} \tag{5}$$

The main purpose of modal analysis is to calculate the eigenvalues and corresponding eigenvectors. The above equation is the characteristic equation of structural vibration. The commonly used methods to calculate eigenvalues in Midas Civil include the eigenvalue vector method and the multiple Ritz vector method. In this section, the Lanczos method in the eigenvalue vector method is used for calculation.

According to the Code for Seismic Design of Buildings [28], in order to accurately analyze the seismic action, the modal participation mass of the structure should reach at least 90%. This paper calculates the first 200 vibration modes of the structure, and the cumulative modal participation mass of X, Y, and Z directions reaches 99.5%, 99.6%, and 96.2%, respectively, meeting the requirements of the code. Due to the limited space, the first 10 order frequencies and modes of the structure are selected, and the results are shown in Table 5.

Table 5. First 10 natural vibration frequencies of the structure.

Modal Order	Frequency (Hz)	Period (s)	Modal Order	Frequency (Hz)	Period (s)
1	0.517	1.934	6	1.168	0.856
2	0.735	1.360	7	1.489	0.671
3	0.767	1.304	8	1.635	0.612
4	1.020	0.980	9	1.735	0.576
5	1.057	0.946	10	1.841	0.543

5. Seismic Response Time History Analysis

The average intensity of an earthquake at the bridge site is 7 degrees, the peak acceleration of ground motion is 0.1 g, and the category of the engineering site is class III. This paper selects a Taft wave suitable for this type of site as the ground motion input. On the basis of the selected seismic wave, the seismic wave is adjusted according to the design of working conditions, and the basic principle of acceleration value adjustment is as follows: the peak value of the actual seismic wave is the same as that of the time–history analysis method (see Formula (6)). In this paper, a total of 7 degrees is applied (the peak value of the design acceleration is 0.35 m/s^2). The revised time–history curve is shown in Figure 7.

$$\acute{a}(t) = \frac{A'_{max}}{A_{max}} \tag{6}$$

where $\acute{a}(t)$ is the adjusted acceleration time–history curve, $a(t)$ is the actual seismic wave before adjustment, A'_{max} is the peak acceleration of the adjusted acceleration curve for time–history analysis, and A_{max} is the peak acceleration of the acceleration time–history curve used for time–history analysis before adjustment.

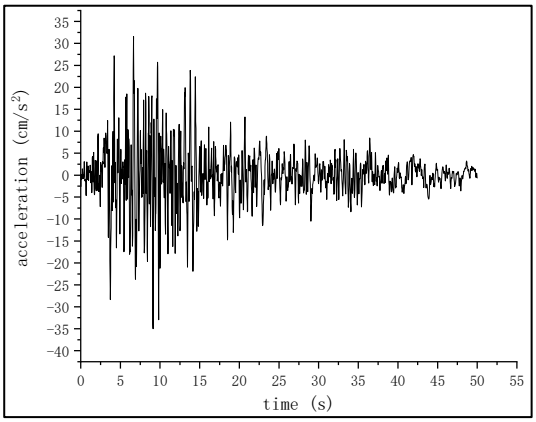
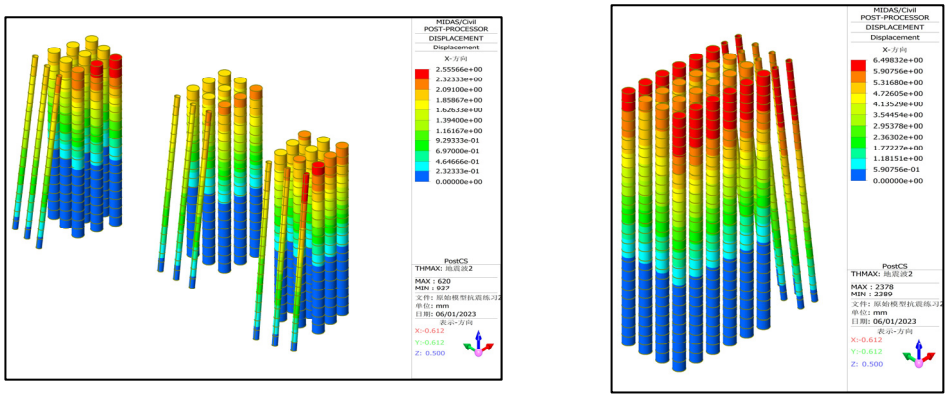


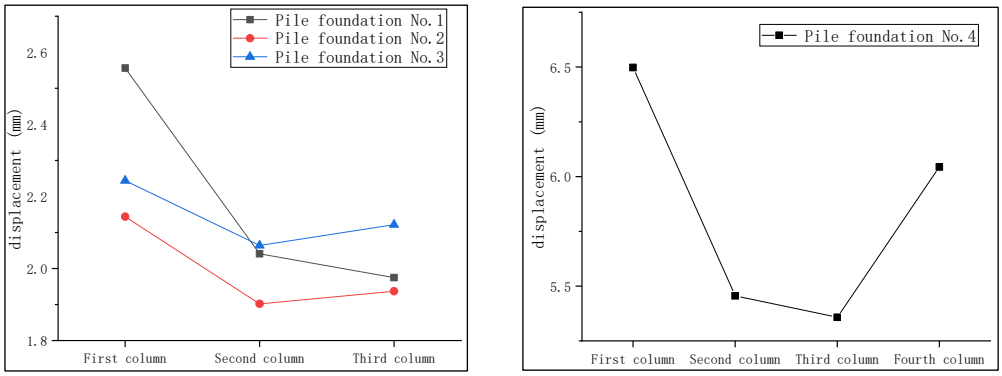
Figure 7. Corrected Taft wave.

According to the selected and adjusted seismic waves, the three-way combined input can be used to obtain the top displacement of each single pile in the pile group foundation, and the results are shown in Figure 8. In addition, the maximum displacement of each column of piles is shown in Figure 9.



(**a**) (**b**)

Figure 8. Pile displacement cloud map: (**a**) #1~#3 pile groups; (**b**) #4 pile group.



(**a**) (**b**)

Figure 9. Maximum displacement diagram of pile top: (**a**) #1–#3 piles top; (**b**) #4 pile top.

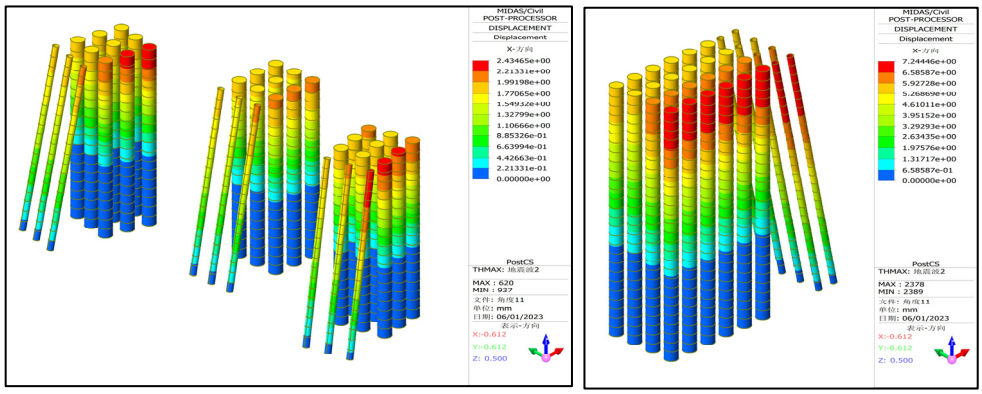
Figures 8a and 9a show the #1, #2, and #3 pile foundations from left to right, respectively. Under the action of earthquake, the displacement of the pile top of the column near the negative direction of Y of each pile group from #1 to #3 changes greatly, and the displacement of pile top reaches the maximum value. The maximum displacements of single pile tops in the #1, #2, and #3 pile groups are 2.556 mm, 2.144 mm, and 2.478 mm, respectively. In addition, the displacement trend of the corresponding single pile along the pile body is roughly the same among the pile groups. At the same time, due to the small depth of the inclined pile embedded in the sandstone, there is still a small amount of horizontal displacement near the bottom of the inclined pile, but the overall displacement trend is still similar to that of the straight pile group.

It can be seen from Figures 8b and 9b that the horizontal displacement of piles on both sides of pile group #4 is slightly larger than the horizontal displacement of piles in the middle two rows. Due to the greater load at #4, the maximum displacement of pile body is greater than from #1 to #3, which is 6.498 mm. The forces of the piles in the back row decrease in turn, but the displacement difference is small, and the maximum difference is 0.043 mm, which can be considered very close. There is still a small amount of horizontal displacement in the bottom part of the inclined pile, but the overall displacement trend is still similar to the straight pile group, and the principle is the same as the analysis of #1~#3 pile group.

6. Influence of Pile Tilt Angle on Seismic Response

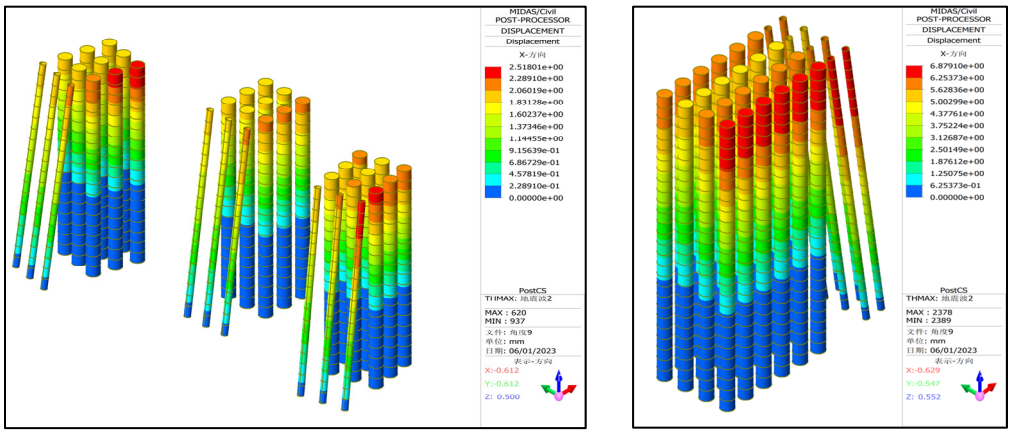
In this paper, the angle between the direction of inclined pile and the direction of gravity is 7°. In order to study the influence of pile inclination on the seismic response of inclined pile group, this paper keeps other parameters unchanged and selects four angles,

namely 3°, 5°, 9°, and 11°, to analyze the influence of angle changes on pile displacement under earthquake action. The calculation results are shown in Figures 10–13. In addition, the variation of pile top displacement with the inclined pile angle is shown in Figure 14.



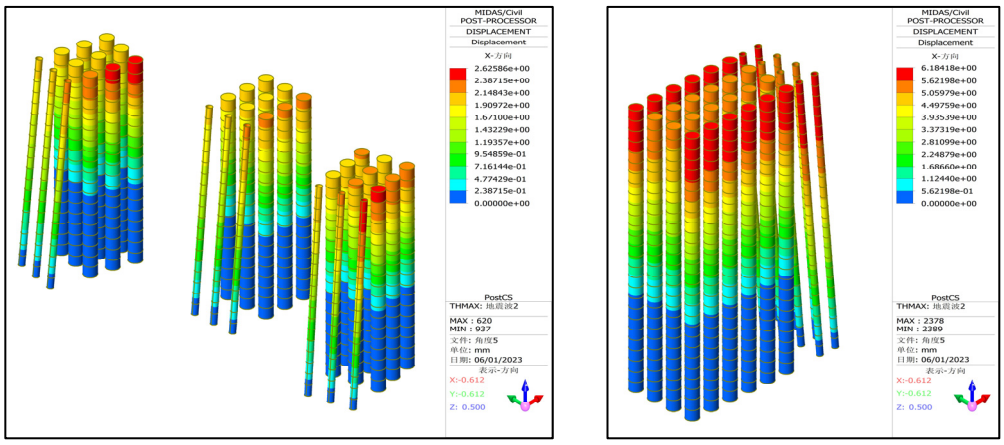
(**a**) (**b**)

Figure 10. Pile displacement cloud map when the tilt angle of inclined pile is 11°: (**a**) #1~#3 pile group; (**b**) #4 pile group.



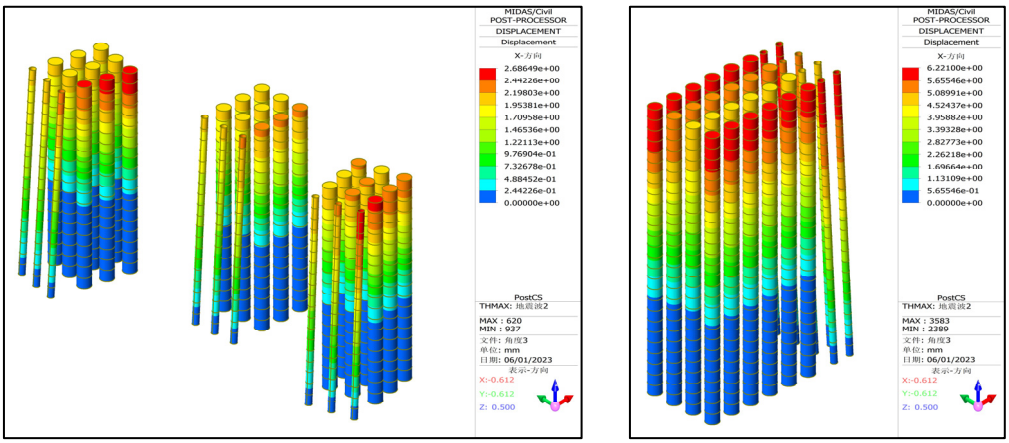
(**a**) (**b**)

Figure 11. Pile displacement cloud map when the tilt angle of pile is 9°: (**a**) #1~#3 pile group; (**b**) #4 pile group.



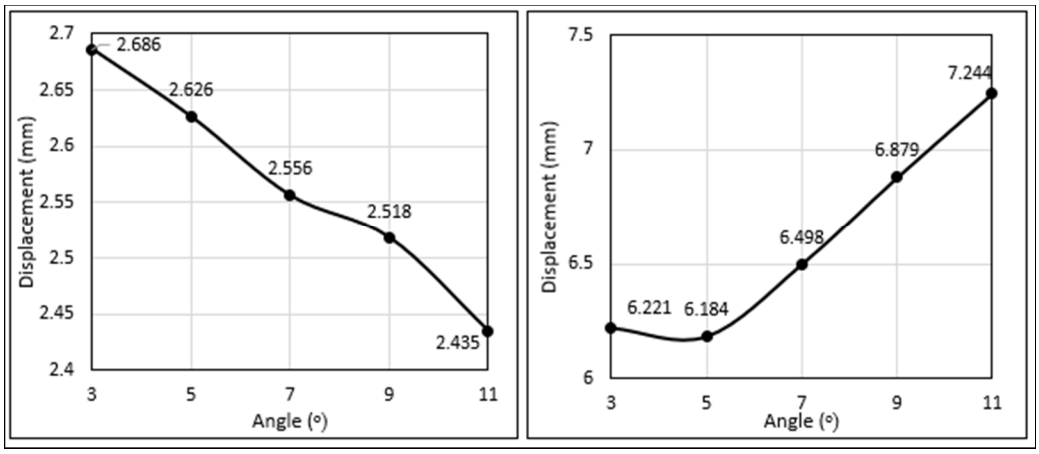
(**a**) (**b**)

Figure 12. Pile displacement cloud map when the tilt angle of pile is 5°: (**a**) #1~#3 pile group; (**b**) #4 pile group.



(**a**) (**b**)

Figure 13. Pile displacement cloud map when the tilt angle of pile is 3°: (**a**) #1~#3 pile group; (**b**) #4 pile group.



(**a**) (**b**)

Figure 14. Pile top displacement diagram varying with inclination angles: (**a**) maximum displacement of #1~#3 pile top; (**b**) maximum displacement of #4 pile top.

As can be seen from Figures 10–13, the overall displacement of #1~#3 pile group foundation is stable with the change in pile body as the angle of inclined pile gradually increases, but the displacement of pile top gradually decreases with the increase in angle, indicating that the increase in inclined pile angle improves the seismic performance of the #1~#3 pile foundation. In the process of increasing the angle of pile group #4 (assuming that each column along the positive direction of Y successively represents the first, second, third, and fourth columns, the top displacement of piles in the first and second columns gradually increases, while that of the third and fourth columns gradually decreases. When the tilt angle is 5–7°, the top displacement of each single pile in pile group is close, indicating that the force of pile group #4 is more uniform. Furthermore, as can be seen from Figure 14, when the inclination is 5°, the displacement of the pile top is small, which is conducive to the resistance of pile foundation #4 to the deformation caused by earthquakes.

7. Conclusions

In this paper, the seismic response of inclined straight pile group foundation of this type of special arch bridge was studied and analyzed, the working characteristics of inclined straight pile group during earthquakes were examined, and the influence of different inclined pile angles on the ability of pile group foundation to resist the deformation caused by earthquakes were discussed. The main conclusions are as follows:

Under the action of earthquakes, the deformation resistance of the #1–#3 pile group foundation is gradually enhanced with the increase in inclined pile angle, which improves the seismic performance of the pile foundation to a certain extent. The deformation resistance of the #4 pile group foundation shows a trend of decreasing first and then increasing with the increase in inclined pile angle, and the horizontal deformation resistance is better when the inclination is 5°.

Under the action of earthquakes, when the inclination angle is 5–7°, the pile top load distribution of the #4 pile group foundation is more uniform, which is conducive to the interactions of each single pile. Therefore, the inclination angle of the inclined pile group foundation of the bridge type should be set within a suitable range.

Author Contributions: Conceptualization, H.Q., W.H., M.A., Z.W., H.W. and J.L.; formal analysis, H.W. and M.A.; investigation, H.Q., H.W. and M.A.; writing—original draft preparation, M.A., H.W. and H.Q.; supervision, H.Q. All authors have read and agreed to the published version of the manuscript.

Funding: The publishing of this paper is financially supported by the National Natural Science Foundation of China (No. 11672215).

Data Availability Statement: The data presented in this study are available on request from the corresponding author.

Conflicts of Interest: The authors declare no conflict of interest.

References

1. Dong, F.; Ning, X.; Zhang, Q. Application and discussion of Straight inclined pile group foundation in Rein-forced concrete arch bridge. *China Water Transp.* **2019**, *19*, 186–188.
2. Saitoh, M.; Padrón, L.A.; Aznárez, J.J.; Maeso, O.; Goit, C.S. Expanded superposition method for impedance functions of inclined pile groups. *Int. J. Numer. Anal. Methods Geomech.* **2016**, *40*, 185–206. [CrossRef]
3. Dai, W.; Shi, C.; Tan, Y.; Rojas, F. A numerical solution and evaluation of dynamic stiffness of pile groups and comparison to experimental results. *Eng. Struct.* **2017**, *151*, 253–260. [CrossRef]
4. Yuan, L. Model Test and Analysis of Horizontal Load Inclined Pile Foundation. Ph.D. Thesis, Zhejiang University, Hangzhou, China, 2012.
5. Gu, M.; Chen, R.; Kong, L.; Chen, Y.; Zhang, Z. Centrifuge model test of pile behavior of inclined pile group under horizontal eccentric load. *Chin. J. Geotech. Eng.* **2014**, *36*, 2018–2024.
6. Goit, C.S.; Saitoh, M.; Mylonakis, G.; Kawakami, H.; Oikawa, H. Model tests on horizontal pile-to-pile interaction incorporating local non-linearity and resonance effects. *Soil. Dyn. Earthq. Eng.* **2013**, *48*, 175–192. [CrossRef]
7. Theland, F.; Lombaert, G.; Francois, S.; Pacoste, C.; Deckner, F.; Blom, P.; Battini, J.M. Dynamic response of driven end-bearing piles and a pile group in soft clay: An experimental validation study. *Eng. Struct.* **2022**, *267*, 114629. [CrossRef]
8. Li, Y.; Zhang, J.; Chen, H.; Qiang, D.; Wang, Y. Study on the Dynamic Response Characteristics and p–y Curve of Straight and Inclined Pile Groups in Saturated Sands. *Appl. Sci.* **2022**, *12*, 2363. [CrossRef]
9. Qiu, H.; Wu, L.; Fu, Z.; Zhu, W.; Huang, W. Numerical analysis of bearing capacity of inclined pile under inclined Load. *J. Wuhan Univ. Technol.* **2020**, *44*, 794–797+802.
10. Huang, W.; Zhou, Z.; Zhang, C.; Qiu, H. Numerical Simulation Analysis of bearing capacity of inclined pile groups in coastal land Area. *J. Constr. Eng.* **2021**, *35*, 301–306.
11. Qiu, H.; Zhou, Y.; Ayasrah, M. Impact Study of Deep Foundations Construction of Inclined and Straight Combined Support Piles on Adjacent Pile Foundations. *Appl. Sci.* **2023**, *13*, 1810. [CrossRef]
12. Qiu, H.; Wang, H.; Ayasrah, M.; Zhou, Z.; Li, B. Study on Horizontal Bearing Capacity of Pile Group Foundation Composed of Inclined and Straight Piles. *Buildings* **2023**, *13*, 690. [CrossRef]
13. Dezi, F.; Carbonari, S.; Morici, M. A numerical model for the dynamic analysis of inclined pile groups. *Earthq. Eng. Struct. Dyn.* **2016**, *45*, 45–68. [CrossRef]
14. Shao, G.; Liu, J.; Wang, T.; Liu, Y. Study on the Bearing Capacity of High-Cap Inclined Pile Foundations. *Adv. Civ. Eng.* **2022**, *2022*, 13. [CrossRef]
15. Álamo, G.M.; Martínez-Castro, A.E.; Padrón, L.A.; Aznárez, J.J.; Gallego, R.; Maeso, O. Efficient numerical model for the computation of impedance functions of inclined pile groups in layered soils. *Eng. Struct.* **2016**, *126*, 379–390. [CrossRef]
16. Zhou, D.; Cai, Q.; Wang, C.; Zhu, Q.; Zhou, Y.; Li, L.; Liu, H. Experimental study on horizontal tension response and p-y curve characteristics of negative inclined pile top. *J. Hunan Univ.* **2023**, *50*, 198–207.
17. Chen, W.; Ma, J.; Wang, J.; Wang, M. Shaking Table test on dynamic characteristics of inclined pile foundation in saturated sand under earthquake. *Railw. Eng. Sci.* **2021**, *18*, 1131–1142.

18. Li, Y.; Gong, J. Nonlinear Finite element analysis of seismic response of high pile wharves with and without inclined piles. *J. Water Con. Environ. Eng.* **2011**, *2*, 1–13.
19. Li, Y.; Zhang, J.; Rong, X. Research progress and new problems in seismic resistance of straight inclined pile foundations in liquefied soil. *Earthq. Eng. Eng. Vib.* **2018**, *38*, 171–181.
20. Huang, B.; Liang, Y. Seismic performance analysis of high pile wharf under pile-soil interaction. *China Water Transp.* **2017**, *17*, 174–175.
21. Chen, T. Centrifuge Test and Numerical Analysis of Seismic Performance of Inclined Pile in Liquefaction Site. Ph.D. Thesis, Tsinghua University, Beijing, China, 2018.
22. Yuan, S. Comparative Study on Seismic Performance of Straight Pile and Inclined Pile in Liquefiable Sand. Ph.D. Thesis, Southwest Jiaotong University, Chengdu, China, 2020.
23. Li, Y.; Zou, Z.; Pan, X.; Zhang, Y. Shaking table test and numerical simulation of lateral response of symmetrical double inclined pile. *Earthq. Eng. Eng. Vib.* **2018**, *38*, 221–230.
24. Zhou, S.; Wang, X.; Tian, W.; Du, B. *Bridge Structure Computer: Finite Element Analysis Method and its Application in MIDAS/Civil*; People's Communications Press: Beijing, China, 2013.
25. Dai, G.; Li, D. *Spatial Analysis and Design Method and Application of Bridge Structure*; People's Communications Press: Beijing, China, 2001.
26. *JTG D60-2004*; General Code for Design of Highway Bridges and Culverts. Ministry of Communication (MOC) of China: Beijing, China, 2004. (In Chinese)
27. Rong, H.; Wei, H.; Guo, H.G. Research on Dynamic Properties of Concrete Steel Tubular Arch Bridge Based on ANSYS. *Appl. Mech. Mater.* **2011**, *1366*, 3233–3236.
28. *GB50011 2010*; Code for Seismic Design of Buildings. China Building Industry Press: Beijing, China, 2021.

Disclaimer/Publisher's Note: The statements, opinions and data contained in all publications are solely those of the individual author(s) and contributor(s) and not of MDPI and/or the editor(s). MDPI and/or the editor(s) disclaim responsibility for any injury to people or property resulting from any ideas, methods, instructions or products referred to in the content.